ISBN: 978-3-95450-184-7 doi:10.18429/JACoW-IPAC2018-WEPAL057

METHODS TO DETECT ERROR SOURCES AND THEIR APPLICATION AT THE TPS

C. H. Huang†, P. C. Chiu, Y. S. Cheng, K. H. Hu, C. Y. Wu, K. T. Hsu
NSRRC, Hsinchu 30076, Taiwan

Abstract

For a low-emittance photon light source, beam stability is a very important property to attain a high-quality photon beam. While it is hard to avoid beam perturbations in a storage ring, it is more important to quickly find the source locations and to remove or eliminate the sources as soon as possible. In this report, we develop a method to identify the locations of multiple sources. For a source with a particular frequency, the relative phase between sources can also be obtained. This method has been a useful tool during TPS operation and its methodology and practical applications are described in this report.

INTRODUCTION

The Taiwan Photon Source (TPS) is a 3 GeV light source with an emittance of 1.6 nm-rad operating routinely at the NSRRC [1]. Beam perturbations can occur at any time from, say, malfunction of a power supply or other effects which may destroy beam stability or trip the electron beam. To achieve a high-quality beam, it is important to develop a method to exactly and quickly identify the error sources.

There are many methods to identify error sources by observing the beam position [2, 3]. However, to our knowledge, there are few papers which discuss in detail how to use these methods to identify multiple sources with the same disturbing frequency. In this paper, first the methodology to detect error sources is introduced and second, we discuss the use of response matrix inversion by singular value decomposition to analyze the location of multi-sources. Finally, this approach is compared with other methods.

METHODOLOGY

The first way to identify an error source could be the use of the Floquet transformation. Field errors cause a beam orbit distortion (D) and the quantity D_j/β_j at the j^{th} beam position monitor (BPM) due to the i^{th} kicker is

$$D_j/\sqrt{\beta_j} = \theta_i\sqrt{\beta_i}\cos\left(\pi\nu - \left|\Psi_j - \Psi_i\right|\right)/(2sin\pi\nu). \quad (1)$$

Here β, ψ, ν and θ are the beta function, phase, tune and kicker angle, respectively. The index i varies from 0 to n, where n is the total number of field errors or orbit kicks. Plotting the function $D_j/\sqrt{\beta_j}$ vs. Ψ_j would represent a pure cosine function with n non-differentiable points at $\Psi_j = \Psi_i$, where the kick or perturbation is located. In this method, it is generally quite easy to identify a single error source even in the presence of some noise in the beam position measurements. Yet, if there are more than three sources or any two sources are too close, it would be very hard to identify the exact location.

Another approach is to use the most effective correctors or MICADO method to identify error sources. The relation between corrector strength and beam orbit distortion can be written as $\boldsymbol{B} = \boldsymbol{RC}$, where $\boldsymbol{R}$ is the response matrix, $\boldsymbol{C}$ is the corrector strength of the correctors and $\boldsymbol{B}$ is the beam orbit distortion. When m correctors are used to correct the beam distortion, the residual beam distortion after correction is $\boldsymbol{r_m} = \boldsymbol{B} - \boldsymbol{R_m C_m}$. The corrector strength to minimize the beam distortion would be the solution ($\boldsymbol{C}_m$) of $\boldsymbol{R_m^T B} - \boldsymbol{R_m^T R_m C_m} = 0$. The root-mean-square (RMS) of the residual orbit is $|r|^2_{min} = \boldsymbol{B^T B} - \boldsymbol{C_m^T R_m^T B}$ and to find the most effective corrector, the variance $|r|^2_{min}$ of each corrector must be calculated where the lowest value indicates the most effective corrector. Calculating the most two effective corrector indicates calculating the variance for each pair of correctors and identifying the pair which results in the smallest RMS residual orbit distortion. Here one of these two correctors is the most effective corrector which is obtained in the previous step. Similar method can be used to calculate the third most effective correctors and so on.

The third method is to use the inverse response matrix method (IRMM) to calculate errors sources. From the measurement of the orbit distortion ($\boldsymbol{B}$) and response matrix ($\boldsymbol{R}$), the error sources should be ideally identified by $\boldsymbol{C}=\boldsymbol{R}^{inv}\boldsymbol{B}$. However, there always exist errors in the orbit and response matrix measurements. These can lead to singularities resulting in unreasonably large and competing corrector strengths caused mostly by noise rather than error sources. Therefore, we use singular value decomposition (SVD) to rewrite the response matrix as $\boldsymbol{R}=\boldsymbol{USV}^T$ [4-6]. The corrector strengths are then $\boldsymbol{C}=\boldsymbol{VS}^{inv}\boldsymbol{U}^T\boldsymbol{B}$, where

$$S_{jj}^{inv} = \begin{cases} 0, & S_{jj} < \varepsilon \\ 1/S_{jj}, & others \end{cases}. \quad (2)$$

The singularity rejection parameter (ε) depends on the signal to noise ratio (S/N) and for a low S/N ratio, ε should be larger to get a better result.

Note that these three methods depend on the machine model. They would not work well as the error sources make huge change of betatron tune.

ANALYSIS IN THE INVERSE RESPONSE MATRIX METHOD

At the TPS we use 167 BPMs (24*7-1) and 168 (24*7) correctors [7] to identify the sources and the eigenvalues of the response matrix are shown in descending order in Fig. 1. As an example, we consider a 1 μrad kick on the orbit by the 53th corrector and a 5% error in the beam orbit measurements. Fig. 2 shows the result of error source detection for different singularity rejection parameters. As

† huang.james@nsrrc.org.tw

ISBN: 978-3-95450-184-7 doi:10.18429/JACoW-IPAC2018-WEPAL057

the rejection parameter increases, which means fewer eigenvalues are used, the results show a broad peak around the source which does not allow the exact identification of the error location. On the other hand, as the rejection parameter is set too low, several peaks appear due to noise. Fortunately, in a realistic case, the orbit measurement errors are much smaller than 5% and there exists a large range to choose the rejection parameter which can give good results.

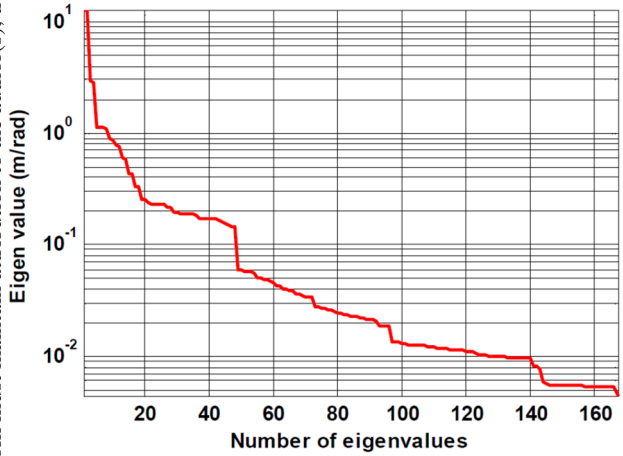

Figure 1: Eigenvalues, in descending order, for the TPS vertical response matrix.

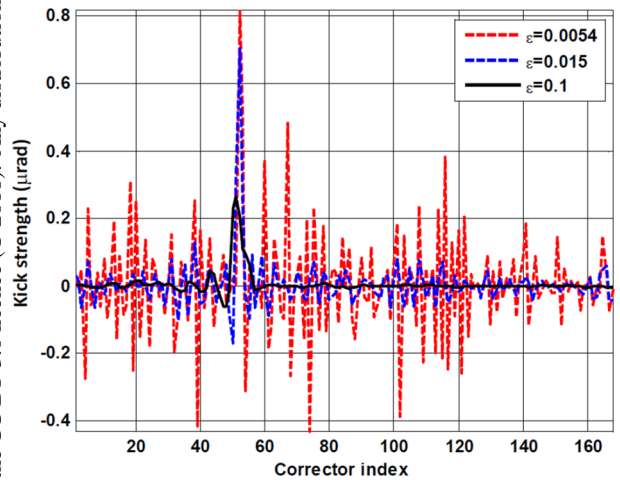

Figure 2: Error-source detection results from response matrix inversion by singular value decomposition with different singular rejection parameters.

BEAM DISTORTION DUE TO THE 2ND KICKER IN THE BOOSTER

After a long shutdown in the winter of 2017, we observed a transient vertical beam perturbation just before injection, which can also be observed by a drop of the photon flux in beam lines. The maximum beam distortion is 40 μm as shown in Fig. 3 (a), with a pulse width around 200 micro second. To find the source, the IRMM is used and the result is shown in Fig. 3 (b) indicating that the source is located near the 1st and 7th corrector in the 23th cell. The only pulsed devices in this region are the extraction kickers and septa of the booster ring. To identify the offending device, the triggers for these components are turned on one by one and finally we found that the perturbation comes from the 2nd kicker magnet.

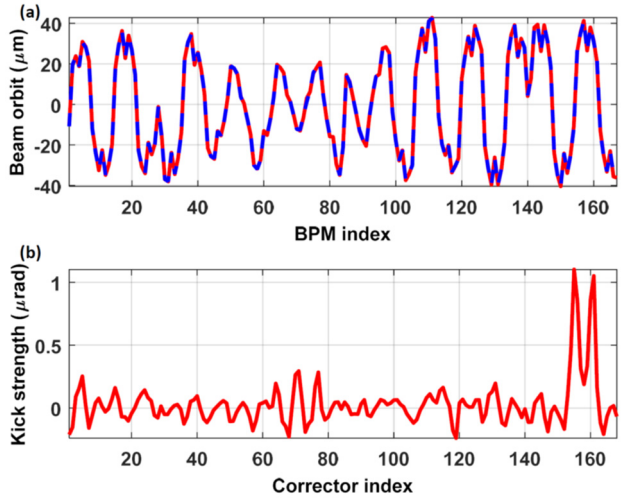

Figure 3: Beam perturbation (a) and error location (b) before the beam injection point.

ERROR SOURCES FOR A PARTICULAR FREQUENCY WITH IRMM

To identify an oscillating error source at a particular frequency, the beam motion at all BPMs must be recorded simultaneously for a particular period. By a Fourier transform of the beam position, we obtain the values of the beam motion at the frequency of interest in each BPM, $B(f) = \int_0^T b(t)e^{-i2\pi ft}dt$. Note that the results of the Fourier transform are in general complex numbers. We follow two methods for the data analysis. The beam orbit should be a real number and the real part of $B(f)$ is the beam orbit at the interesting frequency(f) at zero phase. However, we cannot always expect maximum beam motion at zero phase. Therefore, in the first method, the phase (ϕ) must be varied from 0 to 2π to find the maximum real value of $(B(f)e^{-i\phi})$, and this phase ϕ corresponds to the phase of the source. On the other hand, when the real part $(B(f)e^{-i\phi})$ at a particular phase is used to detect the source, the results shows the error source distribution at that phase. In the second method, the complex values of the Fourier transform are used to identify the sources where the corrector kick angles would be a complex number as well and written as $A_c exp(i\phi_c)$. Here A_c is the corrector kick angle and the ϕ_c is the phase.

ERROR DETECTION OF A 60 HZ BEAM MOTION WITH IRMM

At the beginning of routine operation, the beam was strongly affected by a 60 Hz perturbation [8]. To identify the location of the source, the magnitude of the 60 Hz beam motion is obtained by a Fourier transform. We used both, the real and complex number methods, to identify the source of the 60 Hz beam motion, as shown in Fig. 4 and 5. Both methods show that the perturbation comes from the

ISBN: 978-3-95450-184-7 doi:10.18429/JACoW-IPAC2018-WEPAL057

area at corrector # 105 and 119 which are nearby two radio frequency (RF) cavities. As discussed in the previous section, it takes some time to vary the phase in the first method (using the real part of the orbit spectrum). It is therefore more convenient to use the second method (using complex numbers of the orbit spectrum). To confirm that the error comes from the RF system, one transmitter of the RF cavity was turned off, the beam orbit distortion decreased and the error source near the cavity disappeared in the analysis.

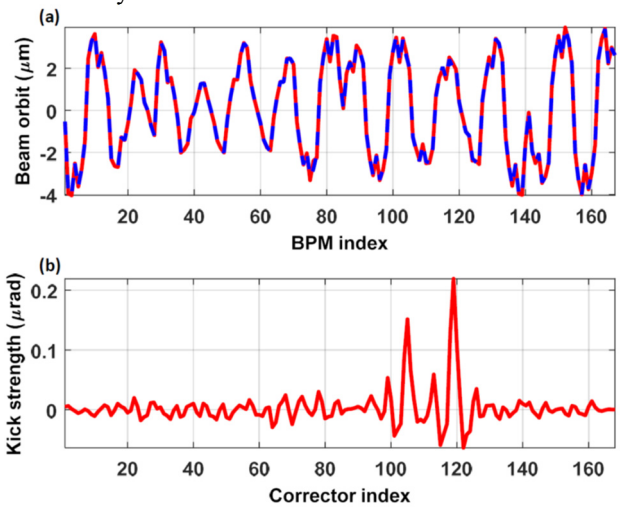

Figure 4: Source detection of a 60 Hz beam motion based on real numbers for the Fourier spectrum.

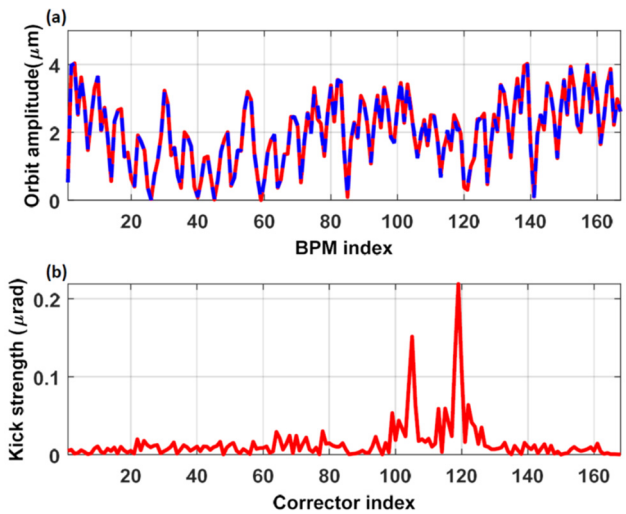

Figure 5: Source detection of a 60 Hz beam motion based on complex numbers for the Fourier spectrum.

COMPARSION BETWEEN IRMM AND OTHER MTHODS

In the previous case, it is very hard to use the Floquet transform to exactly identify the source because these two sources are quite close. Using the MICADO method with two correctors, the sources will point to corrector #111 and #119 rather than #105 and # 119, as the red line shows in Fig. 6. The largest two peaks point to # 105 and #119 only when more than five correctors are used. Beam orbit measurement errors and other minor signals cause the most effective correctors not to be correlated to the actual error sources when only two correctors are used although this drawback can be corrected by increasing the numbers of used correctors. However, as too many correctors are used, the matrix inversion become problematic. Correcting noise and matrix inversion singularity can lead to competing high kick angles in areas far from error locations. Therefore, IRMM with SVD becomes our preferred solution.

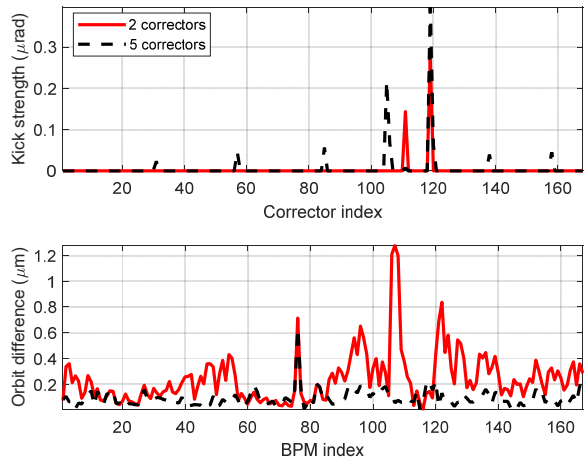

Figure 6: Source detection results of a 60 Hz beam motion in the TPS with MICADO.

CONCLUSION

We compare three methods to identify the location of errors sources and conclude that the response matrix inversion method with singular value decomposition is the most efficient way to locate perturbations from precise beam position measurements. For beam motion at a particular frequency, the phase differences between sources can be obtained as well by this method. This method has been successfully used to identify error locations such as a 60 Hz beam motion caused by the RF system and a vertical beam distortion before injection.

ISBN: 978-3-95450-184-7 doi:10.18429/JACoW-IPAC2018-WEPAL057

REFERENCES

[1] C.C. Kuo, et al., "Commissioning of the Taiwan Photon Source", in *Proc. IPAC'15*, Richmond, USA, paper TUXC3, pp. 1314–1318.

[2] Y. Chuang, et al., "Closed orbit correction using singular value decomposition of the response matrix", in *Proc. PAC'93*, Washington, USA, pp. 2263–2265.

[3] B. Autin and Y. Marti, "Closed orbit correction of A. G. machines using a small number of magnets", in CERN report ISR-MA/73-17.

[4] E. Plouviez, et al., "Optimisation of the SVD treatment in the fast orbit correction of the ESRF storage ring", in *Proc. IBIC'13*, Oxford, UK, paper WEPC13, pp. 694–697.

[5] L. Emery, "Dispersion and betatron function correction in the Advanced Photon Source storage ring using singular value decomposition", in *Proc. PAC'99*, New York, USA, pp. 401–403.

[6] T. Persson, R. Tomas, "Improved control of the betatron coupling in the Large Hadron Collider", Phys. Rev. ST Accel. Beams 17 (2014) 051004.

[7] P.C. Chiu "Fast orbit feedback scheme and implementation for Taiwan Photon Source", in *IPAC'13*, Shanghai, China, paper TUOCB202, pp. 1146–1148.

[8] C.H. Huang, et al., "Study of 60 Hz beam orbit fluctuations in the Taiwan Photon Source", in *Proc. IPAC'17*, Copenhagen, Denmark, paper TUPAB107, pp. 1566–1569.